JSHC
Japan Society of
Histochemistry and Cytochemistry
Established 1959

Acta Histochem. Cytochem. 44 (3): 141–153, 2011
doi:10.1267/ahc.11013

Steady and Temporary Expressions of Smooth Muscle Actin in Hair, Vibrissa, Arrector Pili Muscle, and Other Hair Appendages of Developing Rats

Kiyokazu Morioka[1,2], Mary Arai[3] and Setsunosuke Ihara[3,4]

[1]Laboratory of Electron Microscopy, The Tokyo Metropolitan Institute of Medical Science, Honkomagome, Bunkyo-Ku, Tokyo, Japan, [2]Department of Bioengineering, School of Bioscience and Biotechnology, Tokyo Institute of Technology, Ookayama, Meguro-Ku, Tokyo, Japan, [3]Division of Resources Life Science, The United Graduate School of Agricultural Sciences, Tottori University, Tottori-City, Tottori, Japan and [4]Department of Biological Science, Faculty of Life and Environmental Science, Shimane University, Matsue, Shimane, Japan

Received March 31, 2011; accepted May 24, 2011; published online June 27, 2011

The hair erection muscle, arrector pili, is a kind of smooth muscle located in the mammalian dermis. The immunohistochemical study using an antibody against smooth muscle alpha actin (SMA) showed that the arrector pili muscle develops approximately 1–2 weeks after birth in dorsal and ventral skin, but thereafter they degenerate. The arrector pili muscle was not detected in the mystacial pad during any stage of development, even in the neighboring pelage-type hair follicle. A strong signal of SMA in the skin was located in the dermal sheath as well as in some outer root sheath cells in the hair and vibrissal follicles. Positive areas in the dermal and outer root sheaths were restricted to a lower moiety, particularly areas of similar height, where keratinization of the hair shaft occurs. This rule is valid for both pelage hair follicles and vibrissal follicles. At medium heights of the follicle, SMA staining in the dermal sheath was patchy and distant from the boundary between dermis and epidermis. In contrast to SMA, vimentin was expressed over the entire height of the dermal sheath. Unlike the arrector pili muscle, the expression of SMA in the dermal sheath was observed during fetal, neonatal, and adult stages. The presence of actin-myosin and vimentin fibers in supporting cells is thought to be beneficial for the hair follicle to cope with the movement of the hair shaft, which may be caused by physical contacts with outside materials or by the contraction of internal muscles.

Key words: hair, arrector pili muscle, smooth muscle actin, vimentin, dermal sheath

I. Introduction

The hair shaft consists of only epidermal tissues, but is supported by not only epidermal inner and outer root sheaths but also basement membrane, dermal tissues, appendages, and multiple types of other non-epidermal cells for its development, growth, differentiation, nutrition, movement, secretion, physical stability, and coloring [10, 11, 17, 18]. The arrector pili muscle is a hair-supporting dermal tissue and a kind of smooth muscle that serves to maintain the warmth of the mammalian body through erecting hairs [4, 28, 32]. The structure of the arrector pili muscle has been reported in the literature with regard to hair [10], dermatology [4, 32], anatomy [28], and zoology [1], although many of the details are still controversial. The morphology of the distal ends of the muscle has been studied by several investigators [2, 21–23], and 3D structure models have recently been presented [26, 27]. Although the distal ends of the arrector pili muscle are drawn as if they adhere closely to the basement membrane beneath the layer of the skin epidermis in most literatures, it is notable that the authors of Gray's anatomy [28] as well as some other papers [22, 23] have illustrated them in a way that shows they are

Correspondence to: Dr. Kiyokazu Morioka, Department of Bio-engineering, School of Bioscience and Biotechnology, Tokyo Institute of Technology, 2–12–1 Ookayama, Meguro-Ku, Tokyo 152–8550, Japan. E-mail: morioka@mbp.nifty.com

not attached directly to the basement membrane. Piloerection has been used as a marker of some toxic agents [14, 25, 30, 31] or brain functions [13, 15]; however, the approaches from developmental and physiological perspectives have provided limited information. Therefore, in the present study we aimed to observe the development of the arrector pili muscle in fetal, neonatal, and adult rats by using immunohistochemical staining techniques using an antibody against SMA, one of the major components of the arrector pili muscle.

Another purpose of this study was to observe smooth muscle α-actin (SMA) and vimentin expressions in the skin and hair follicles. Hair follicle consists of a solid, strong upper structure supported by a soft and weak root structure. Moreover, the upper structure moves vigorously through contact with external objects, while the movement of the root is restricted. To retain a hair follicle to remain uninjured under such circumstances, the hair root has to possess both elasticity and strength, which may be at least partially conferred by smooth muscles and intermediate filaments. The mechanism providing elasticity is thought to be particularly important. We previously investigated actin and myosin localization using antibodies against skeletal muscle and smooth muscle myosins in combination with a pan-actin antibody. Our results suggested that the actin-myosin system is involved in reinforcing the structure and function of skin and hair cells [19]. In addition to intracellular reinforcement, the building of cell-to-cell adhesion systems is also crucial [9, 16], although we did not herein address this issue. Jahoda and colleagues previously observed that SMA is present in the dermal sheath of rat vibrissae, rat pelage, and human follicles [12]. In this study, we confirmed their results and conducted more detailed observations regarding SMA and vimentin localization in the hair and vibrissal follicles located in dorsal skin, ventral skin, and mystacial pad, by using skin obtained from fetal, neonatal, and adult rats.

II. Materials and Methods

Sample preparation

Fourteen-day-old pregnant Sprague–Dawley rats were obtained from Nippon SLC Inc. Treatment of animals was carried out according to the guidelines of our institute, which conform to the principles of laboratory animal care of NIH. The appearance of the vaginal plug was used to indicate day 0 of gestation. Delivery of newborn animals was observed at gestation day 21 or 22. In this paper, day 19F represents gestation day 19, day 0 represents the day of birth, and day 2 represents day 2 after birth. Skin used for immunoblotting was cut into small fragments (approximately 2×5 mm), frozen in liquid nitrogen, and stored at −80°C until use. Fragments for immunohistochemical staining were fixed in 10% formalin neutral buffer solution (Wako Pure Chemical Industries Ltd., Osaka, Japan) for several days at 4°C, dehydrated, and embedded in paraffin. Paraffin blocks were sectioned at 6-μm thickness using a Leica RM2135 microtome (Leica Microsystems AG, Wetzler, Germany).

Primary antibodies

Mouse anti-smooth muscle α-actin monoclonal antibody Ab-1 (clone 1A4) was purchased from Thermo Fischer Scientific Inc. (Fremont, CA). The antibody solution was diluted to 1:800 using 10 mM phosphate buffered saline (PBS) (pH 7.4) containing 0.2% bovine serum albumin (BSA) before use, or Ready-to-Use product was used without dilution. Mouse anti-pig eye lens vimentin monoclonal antibody Ab-2 (clone V9) was also purchased from Thermo Fisher Scientific Inc.

Immunoblotting

Stored frozen samples obtained from the dorsal skin of rats on day 7 after birth were pulverized with a stainless steel rod (SK200; Tokken Inc., Chiba, Japan). The temperature was maintained below freezing during this operation. The powder was then heated at 95°C for 2 min in 125 mM Tris-HCl (pH, 6.8), 4.3% sodium dodecyl sulfate, 10% 2-mercaptoethanol, 30% glycerol, and 0.01% bromophenol blue solution. Polyacrylamide gradient gels (4–20%) for electrophoresis were purchased from Daiichi Pure Chemicals Co., Ltd. (Tokyo, Japan). Immunoblotting ABC-POD kits for mice and rabbits were purchased from Wako. Experiments were performed according to the manufacturer's instructions. Proteins were transferred to a polyvinylidene fluoride (PVDF) membrane at 2 mA/cm^2 for 60 min. Marker proteins were obtained from Thermo Fischer Scientific Inc. Protein bands were stained with Page blue 83 (CBB R-250) obtained from Daiichi Pure Chemicals Co. Ltd.

Immunohistochemistry

Experiments were carried out at room temperature, except incubation with primary antibodies, which was carried out at 4°C. The specimens were dehydrated using a xylene-ethanol series and treated with 3% hydrogen peroxide for 60 min, followed by washing 3 times with PBS. Samples were then incubated with 10% goat serum (Nichirei Co., Tokyo, Japan) for 60 min to block nonspecific staining and washed 3 times with PBS. Incubation of sections with primary antibodies was carried out for 24 hr at 4°C. Sections were then washed 4 times with PBS and subsequently incubated with a secondary antibody for 60 min. We used Histofine Simple-Stain Rat MAX-PO (MULTI) as the secondary antibody, which was obtained from Nichirei Co. (Tokyo, Japan). The MAX-PO consists of a polymer conjugated with Fab secondary antibody and peroxidase. Localizations of the complex were visualized using 3-3'-diaminobenzidine (DAB). The sections colored by DAB were briefly poststained using methylgreen-pyronine [19]. In addition to immunoperoxidase staining, some sections were stained with hematoxylin and eosin for histological examination. An Olympus BX-51 microscope equipped with an Olympus E-420 digital camera system was used to obtain photographs.

III. Results

Immunoblotting

The anti-vimentin antibody reacted only with the protein corresponding to vimentin (Fig. 1, Lane 3). Anti-SMA antibody reacted primarily with the protein corresponding to SMA, but it appeared to react slightly with lower molecular weight proteins as well (Fig. 1, Lane 4). Since the preparations of samples were carried out without thawing before the addition of hot sodium dodecyl sulfate solution, the probability of actin degradation was low in the operation. Nonetheless, it is possible that reactions of the antibody with degraded proteins that preexisted before the operation may have taken place because the skin contains a large amount of dead and dying cells, such as the cornified layer cells of the epidermis and inner root sheath cells of hair follicles, among others, which continually undergo autolysis [20]. Because the signal was negative in various non-muscle tissues as well as adult striated muscles (see for examples, Fig. 2I, 5H, or 8B), we do not think that this antibody reacts with non-muscle actins or striated muscle actins.

Dorsal skin

The area indicated by the arrow in Figure 2A exhibits nonspecific staining and occurs in the experiment in which primary antibody was not used. Because fetal skin from gestation day 16 rats, where the skin had not yet cornified, did not display any nonspecific staining (Fig. 5A), the nonspecific staining is thought to be correlated with a specific cellular state that occurs in preparation for terminal skin keratinization. We have thus excluded a discussion regarding the interfollicular epidermis in this paper.

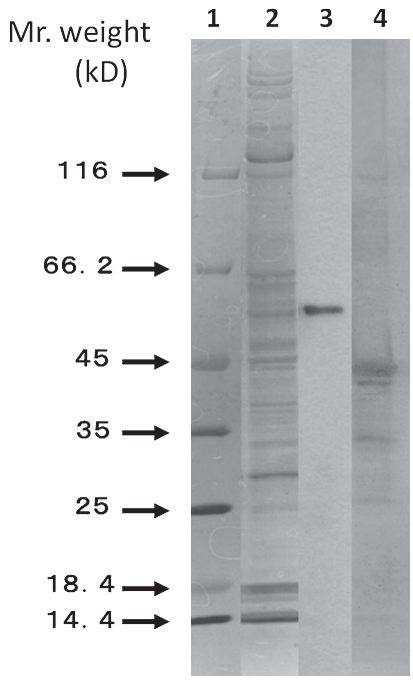

Fig. 1. Immunoblot of skin proteins reacted with antibodies against vimentin and smooth muscle α-actin (SMA). Samples were treated and stained as described in the text. Column 1: Molecular weight markers. Column 2: Staining of proteins by Coomassie brilliant blue R-250. Column 3: Immunoblot staining of vimentin. Column 4: Immunoblot staining of smooth muscle α-actin (SMA).

At day 19F (day 19 of gestation), distinct SMA expression was not detected in the skin, except in some cells of dermal muscle (DM in Fig. 2B). Staining of dermal muscle was more distinct on day 2 after birth (Fig. 2C and 2D), whereas it disappeared on day 35 (Fig. 2H and 2I), suggesting that the contribution of SMA to this tissue is restricted to the neonatal stage or is a vestigial phenomenon. The SMA signal in the dermal sheath of the hair follicle was detected beginning on day 2 after birth (arrows in Fig. 2C and 2D) and persisted throughout the adult stages (arrows in Fig. 2J), although the area is restricted to the lower half of the follicle (arrows in Fig. 2C and 2D). SMA signal was also found in blood vessels (Fig. 2C, * and the inset figure).

Remarkable staining was observed on day 7 (Fig. 2E and 2F) and on day 14 (Fig. 2G) at the interfollicular spaces of the hair follicles. Some of them are indicated by the arrows in these figures. On the basis of their morphology, these tissues were identified as arrector pili muscles (hair erection muscles). In the juvenile animals, the arrector pili muscles and hair follicles were aligned primarily by turns (Fig. 2E–G, Fig. 3). When the animals reach the adult stage (for example, on day 35), the arrector pili muscles appeared to be less vigorous than on day 14 (Fig. 2H). As shown in the next section, degeneration of the arrector pili muscle in adult animals was also observed in the ventral skin.

Through SMA staining, the fine structures of the arrector pili muscle were detectable, as shown in Figure 3. Asterisks in Figure 3 depict the curvature of the muscle, which detours to avoid the sebaceous gland (SG). As shown in Figure 3, the dermal sheath and outer root sheath around the point of contact of the arrector pili muscle showed no signal of SMA. The absence of SMA in this area suggests that the smooth muscle of the dermal sheath does not function to clasp the arrector pili muscle. The arrector pili muscle connects to the dermal sheath and/or outer root sheath in a variety of forms (thick arrows in Fig. 3). The opposite end of the arrector pili muscle is often branched, as designated by the circles in Figure 3. Although we examined many cases, we did not observe the attachment of the arrector pili muscle to the basement membrane, including those cases shown in Figure 3I.

Ventral skin

The staining patterns of SMA in the ventral skin are essentially the same as those in the dorsal skin. No distinct shape of the arrector pili muscle was detectable on day 2 after birth (Fig. 4B), while the full-sized muscles were observed on day 7 (Fig. 4D–4H). No morphological differences were observed between dorsal and ventral arrector

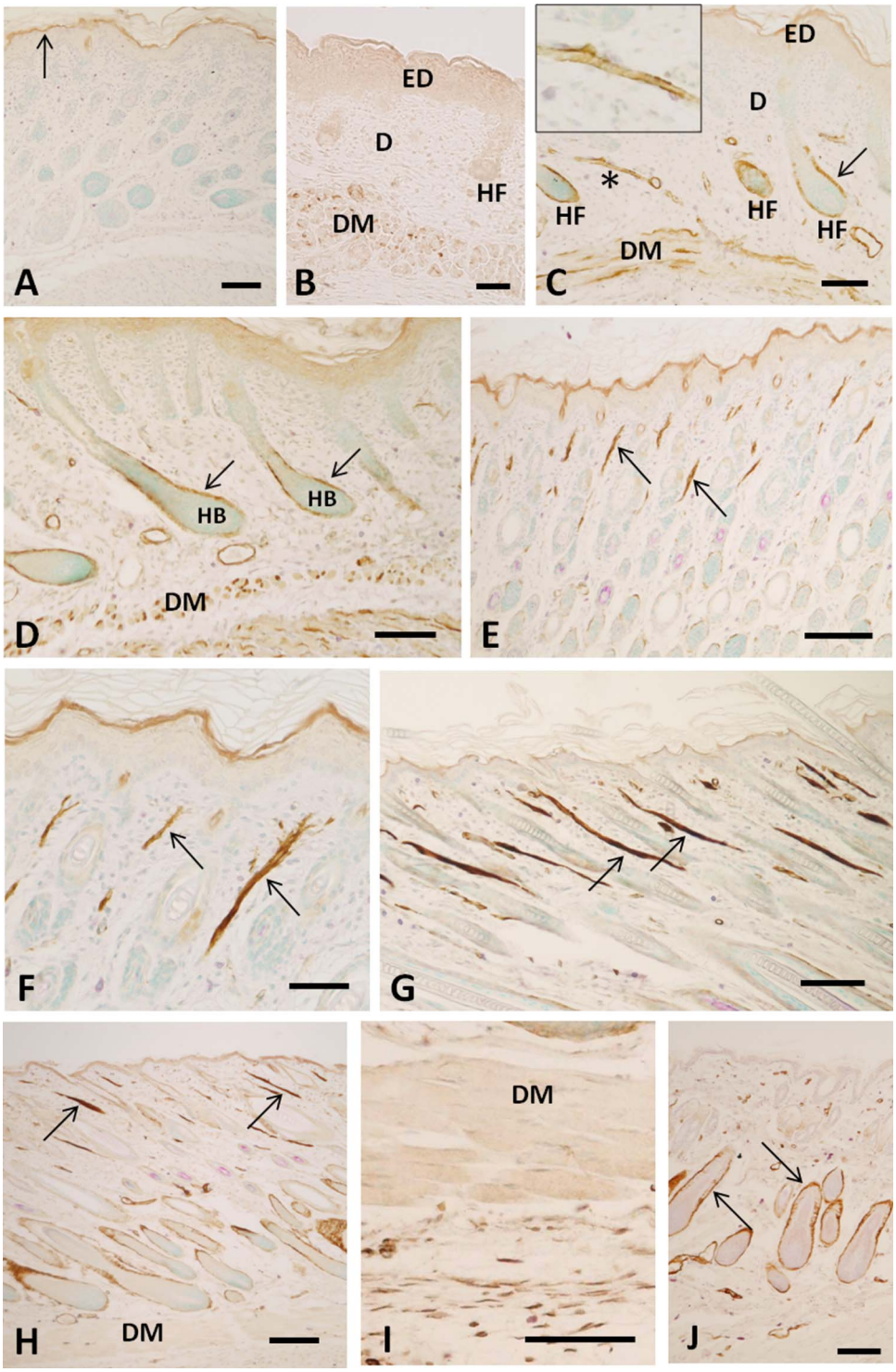

Fig. 2. Localization of SMA in the dorsal skin of fetal, neonatal, and adult rats. (**A**) Control experiment without the reaction with primary antibody (same in the following figures). The arrow indicates nonspecific staining appearing in the innermost area of the cornified skin epidermis layers. No other tissues or cells exhibited this nonspecific staining. The sample was obtained from the rat dorsal skin on day 2 after birth. (**B**) Gestation day 19 (Day 19F). ED, D, HF, and DM represent epidermis, dermis, hair follicle, and dermal muscle, respectively. These abbreviations are also used in the following figures. (**C, D**) Day 2 after birth. Arrows indicate staining of the dermal sheath of the hair follicle. The asterisk in (**C**) designates a thin blood vessel stained by an antibody against SMA. This is also shown in the inset window in (**C**) as an enlarged picture. HB represents the hair bulb. (**E, F**) Day 7 after birth. Arrows in (**E–H**) indicate SMA staining of arrector pili muscle. (**G**) Day 14 after birth. (**H, I**) Day 35 after birth. (**J**) Day 61 after birth. Bars=50 μm (**F**), 100 μm (**A–D, I, J**), and 200 μm (**H**).

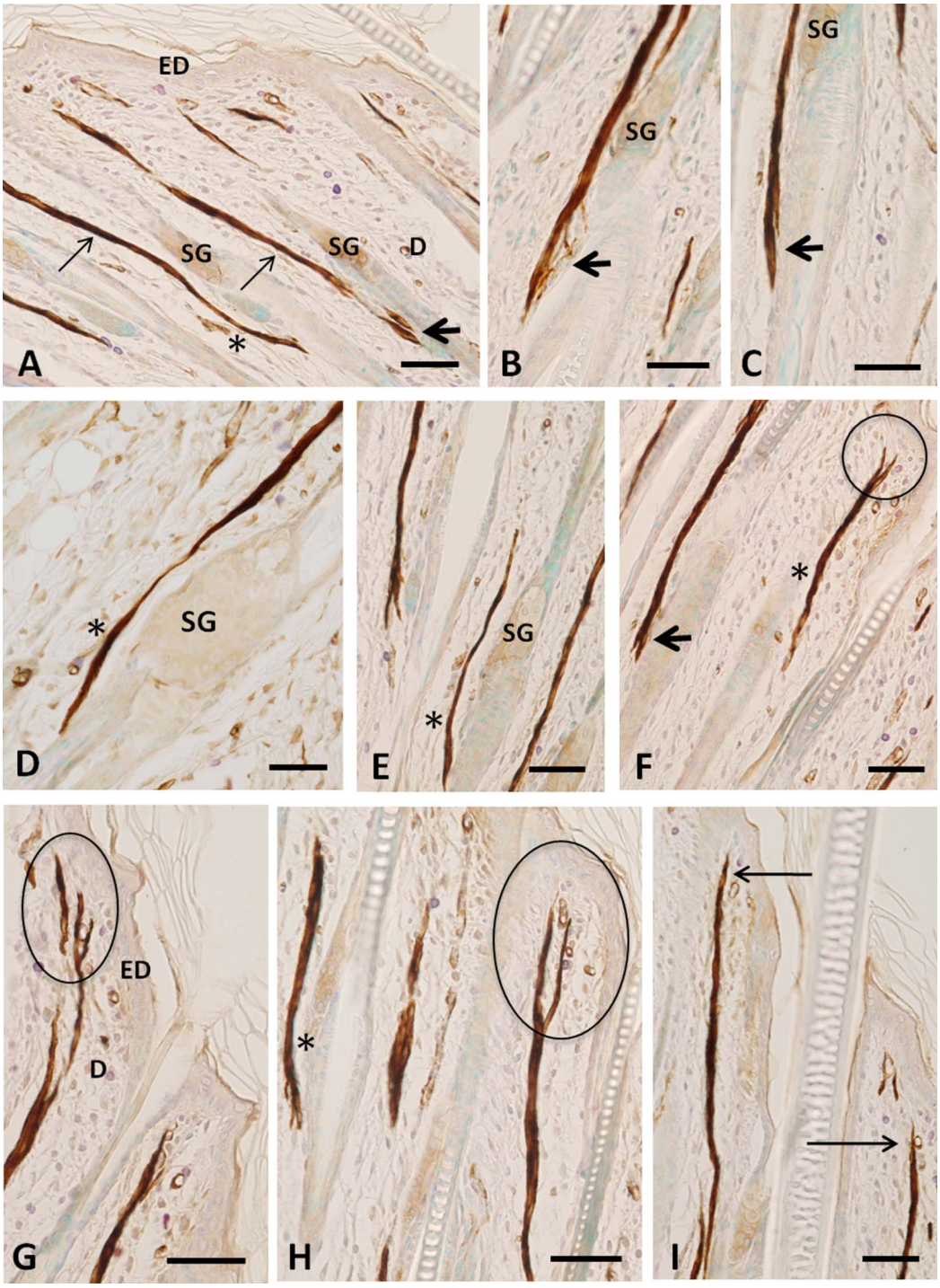

Fig. 3. Morphology of arrector pili muscle revealed by SMA staining in rat dorsal skin on day 14 after birth. ED, D, and SG represent epidermis, dermis, and sebaceous gland, respectively. Thin arrows in (**A**) indicate the arrector pili muscle. Thick arrows in (**A–C, F**) indicate the attachment of the lower ends of arrector pili muscle to the hair follicles. Areas encircled by ellipses in (**F–H**) designate the branched upper ends of arrector pili muscle. The thin arrow in (**I**) indicates the straight upper end of the arrector pili muscle. Asterisks show the position of curvature in arrector pili muscle. Bars=50 μm.

pili muscles (Fig. 4F–4H); however, they were shown to be barely detectable in the ventral skin on day 35 (Fig. 4J). The functional degeneration of the arrector pili muscle was suggested to be more drastic in the ventral skin compared to that in the dorsal skin (Fig. 2H and 4J). Arrows in Figures 4K and 4L designate attenuated SMA staining. Decrease in SMA expression is thought to cause the degeneration of arrector pili muscles.

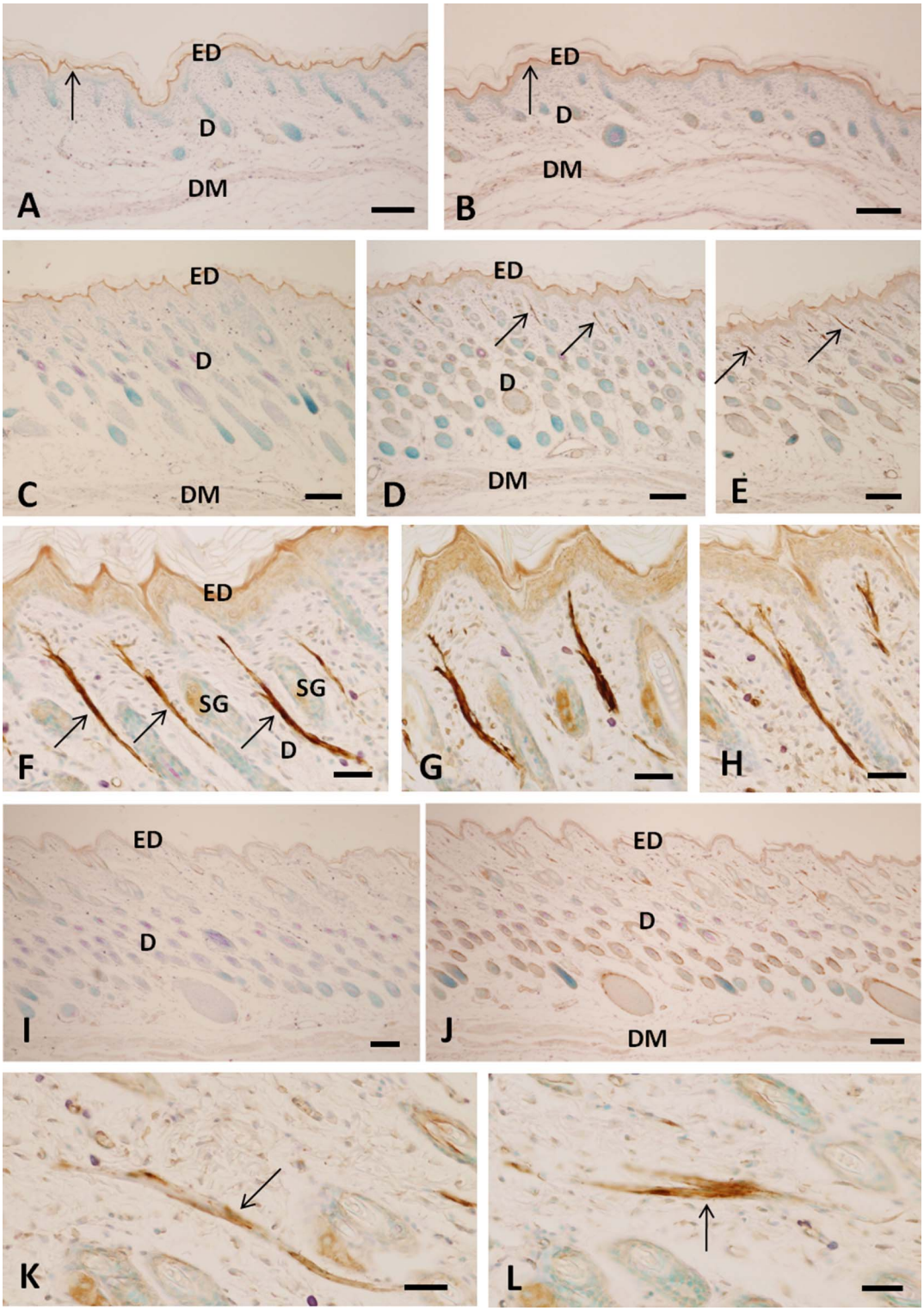

Fig. 4. Localization of SMA in the ventral skin of the rat. Abbreviations are the same as in Figures 2 and 3. (**A**) Control. Arrows indicate nonspecific staining as in Figure 2A. Samples were obtained from the ventral skin of neonatal animals on day 2 after birth. (**B**) Day 2 after birth. (**C**) Control. Day 7 after birth. (**D–H**) Day 7 after birth. Arrows indicate the arrector pili muscle detected by the SMA staining. (**I**) Control. Day 35 after birth. (**J–L**) Day 35 after birth. Arrows in (**K**) and (**L**) show the decline of staining of SMA in arrector pili muscle at this period. Bars=200 μm (**A–E, I**, and **J**), 50 μm (**F, H, K**, and **L**).

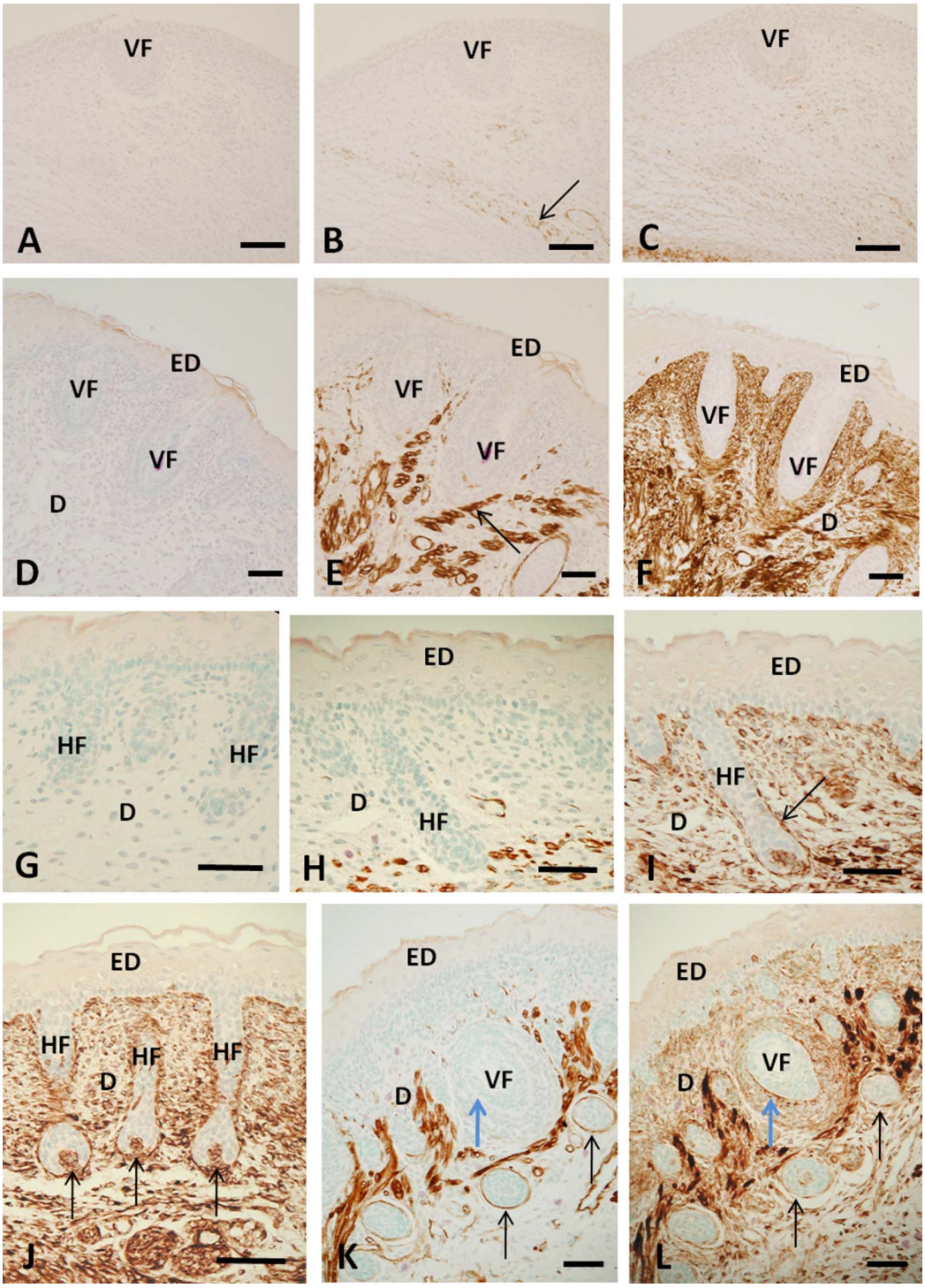

Fig. 5. Localization of SMA and vimentin in the mystacial pad of fetal rats. The abbreviation VF represents the vibrissal follicle. Other abbreviations are the same as those in Figure 2. (**A–C**) Samples were obtained from the mystacial pads of the animals on gestation day 16 (day 16F). (**A**) Control. (**B**) SMA staining. The arrow shows weak staining of the dermal muscle. (**C**) Vimentin staining. (**D–L**) Samples were obtained from the mystacial pads of the animals on gestation day 19 (day 19F). (**D, G**) Control. (**E, H, K**) SMA staining. (**F, I, J, L**) Vimentin staining. The arrow in (**E**) indicates staining of SMA in the dermis. The arrow in (**I**) indicates vimentin staining in the dermal sheath. The arrows in (**J**) indicate vimentin staining in the dermal papilla. The black arrows in (**K**) and (**L**) indicate SMA and vimentin staining in the lower dermal sheath, respectively. Blue arrows in (**K**) and (**L**) indicate SMA and vimentin staining in the upper dermal sheath, respectively. Bars=100 μm (**A–C**), 50 μm (**D–I**).

Mystacial pad in fetus

A primitive vibrissal follicle was surrounded by the multilayered dermal cells in the mystacial pad on day 16F (Fig. 5A–C). Both SMA and vimentin signals in the fetal skin were negative on day 16F, although some undetermined dermal cells (arrow in Fig. 5B) and blood vessel cells exhibited slightly positive signals (Fig. 5B and 5C). In contrast, both signals were increased and were strong and abundant on day 19F. Not only blood vessel cells but also voluntary muscle cells expressed an SMA signal (arrow in Fig. 5E). The position of striated voluntary muscle in the mystacial pad was estimated previously [19]. Unlike SMA, vimentin appears to be pervasively present in the dermal cells (Fig. 5F). In contrast to the staining around the vibrissae, no SMA staining was observed around the pelage-type hair follicle, except for the subcutaneous dermal muscle and blood vessels on day 19F (Fig. 5H). It should be noted that the dermal sheath and dermal papilla in the pelage-type hair follicles were not stained by anti-SMA antibody (Fig. 5H). This pattern of staining was observed only in the skin of fetal animals. On the day 19F, the dermal sheaths surrounding the lower part of vibrissae may express SMA (black arrows in Fig. 5K).

In contrast to SMA, vimentin may be expressed in the dermal sheath (arrow in Fig. 5I) and in the dermal papillae (arrow in Fig. 5J) of pelage hairs on day 19F. Adjacent sections shown in Fig. 5K and Fig. 5L are neighboring. Although the staining of vimentin in the lower dermal sheath is weaker than that of SMA (black arrows in Fig. 5K vs. the corresponding positions in Fig. 5L), the upper area of the dermal sheath is positive for vimentin (blue arrow in Fig. 5L). The staining of SMA was not detectable at the corresponding position (blue arrow) in Figure 5K.

Mystacial pad after birth

Figure 6B shows a mystacial pad section from day 2 after birth, where the vibrissal follicles are displayed in order of development. Muscles driving the vibrissae are located unilaterally, and were shown to be positively stained for SMA (thin black arrows in Fig. 6B and 6C), as well as for the staining of striated muscle actin and myosin (22). Figure 6B also shows that the follicles in the earlier stages (numbered 5–7, thick blue arrows) did not react with the anti-SMA antibody, while in later stages (numbered 1–4, thick black arrows), the vibrissal follicles became positive for SMA staining. SMA staining in these follicles was shown to be restricted to the lower region of the dermal sheath (thick arrow in Fig. 6B). This result was confirmed by results shown in Figure 6C, in which the stained area is designated by a thick black arrow. In addition to the dermal sheath, the striated muscles (thin arrows in Fig. 6C) and a dermal blood vessel (asterisk in Fig. 6C) were positive for SMA. Staining patterns of SMA and vimentin in the hair bulb are shown in Fig. 6D and 6E, respectively. Although SMA staining in the dermal sheath surrounding the hair bulb often appeared to be faint or lost in later stages, staining was evident on day 2 after birth, as shown in Figure 6D. SMA staining in the dermal papilla was negative until blood vessel penetration. As shown in Figure 6E, vimentin staining was shown to be occasionally modest in the dermal papilla, even if the dermal sheath surrounding the hair bulb was distinctly stained. According to the results shown in Figure 6D and 6E, dermal sheath cells may occasionally lose their specific dermal sheath cell characteristics when entering the core of the hair bulb to produce dermal papilla.

SMA staining in the dermal sheath was restricted to the area associated with lower part of the pelage-type (nonvibrissal) follicles as well as the vibrissal follicles on day 2 after birth (Fig. 6F; see also Fig. 6H and 6I). Except for immature or tiny follicles, this staining pattern appears to be general. It appears that some small hair follicles, such as (c) in Figure 6H, were not accompanied by a positive SMA signal in the dermal sheath. Figure 6I shows that an outer root sheath does not express a distinct SMA signal, though it expresses the signal in later stages. Vimentin is ubiquitously expressed in the dermal cells, including the dermal sheaths of hair follicles (Fig. 6G). However, the dermal sheath wrapping the hair bulb often lacks a vimentin signal (Fig. 6G and 6L). The expression of SMA seemed to be strongest in the areas just above the hair bulb (Fig. 6F). Vimentin expression of dermal sheath was low in the area surrounding the hair bulb (blue arrow in Fig. G). These results suggest that the hair bulb may not be significantly affected by the physical stress induced by hair shaft bending, compared to the area just above the hair bulb. Figures 6K and 6L show that the dermal papillae typically express a vimentin signal, whereas they do not express an SMA signal.

Figure 7A shows the longitudinal section of a vibrissal follicle stained using an immunohistochemical kit of SMA antibody in the adult animal on day 42 after birth. In addition to the typical pelage-type hair components (hair shaft, epidermal inner and outer root sheaths, and dermal sheath), the vibrissa includes the ring sinus, cavernous sinus, ringwulst, vibrissal capsule (Fig. 7A), and nerve fibers (see Fig. 7C, where DVN means deep vibrissal nerve). The vibrissa capsule is typically very thick, but it is thin near the bottom area of the follicle and it expresses SMA, unlike other areas of the capsule (Figs. 7A, 7B, 7G, 8C). The presence of SMA is typical of ordinary blood vessels. SMA staining in the dermal sheath is shown to be positive in the level lower than the cavernous sinus (CS) (Fig. 7A and 7C), partially positive at the same level as CS (Fig. 7A and 7D), and negative at a level higher than the CS (Fig. 7A and 7E). In adult animals, the vascular system often enters into the dermal papilla, resulting in SMA expression (Fig. 7G). In contrast to SMA, vimentin staining is typically pervasive in the dermal papilla (Fig. 7H). Nevertheless, some dermal papillae had no vimentin signal (data not shown). We did not attempt to determine the reason for this variation.

The outer root sheaths of some hair follicles show a strong SMA signal, as designated by (a) in Figure 7I. The area of the outer root sheath located just above the vibrissal hair bulb may typically retain the SMA signal (Figs. 7J, 7L, 8E), although the companion layer (CP in Fig. 7L) appears

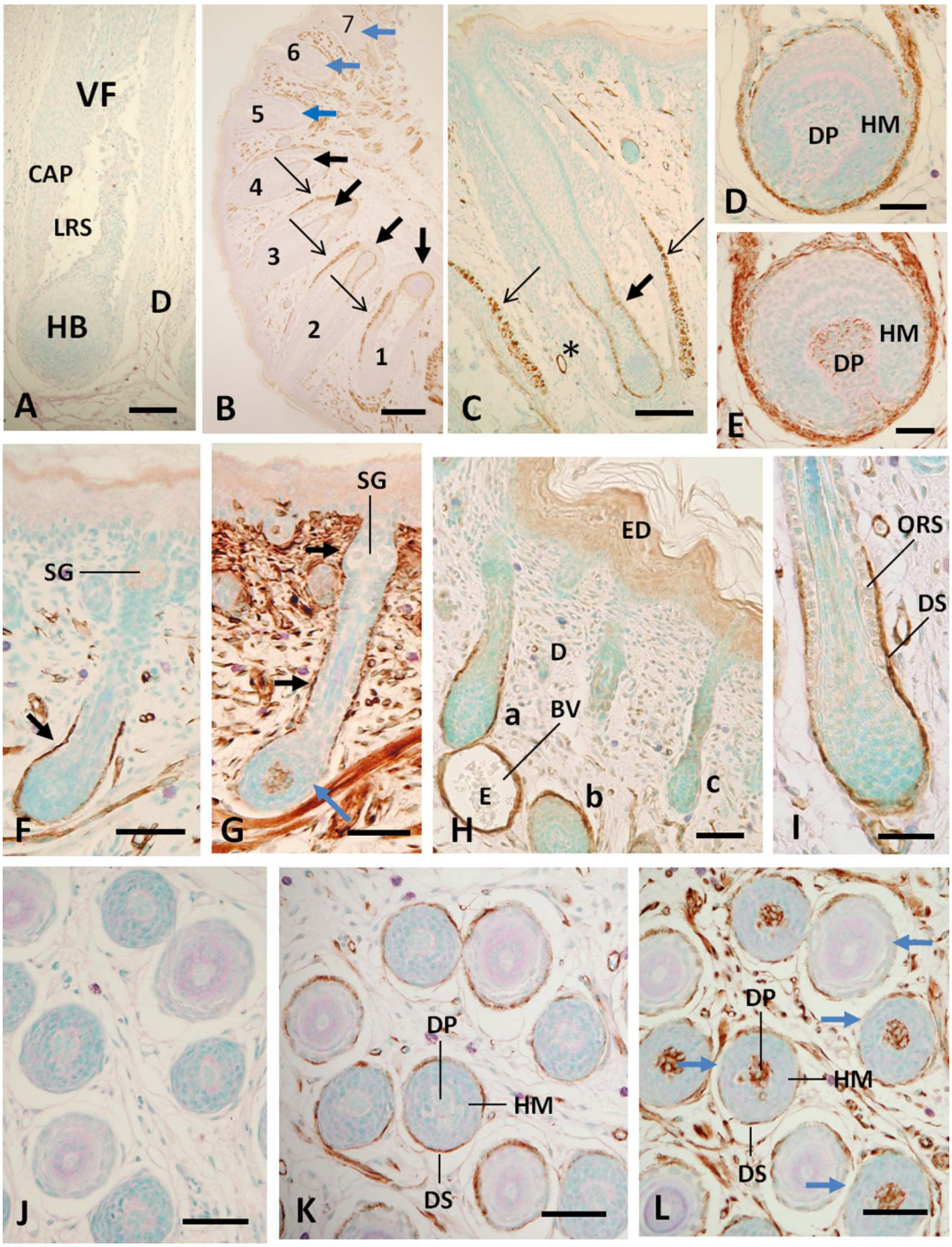

Fig. 6. Localization of SMA and vimentin in the mystacial pad of neonatal rats. The abbreviations, CAP, LRS, HB, HM, BV, E, and ORS represent the capsule of vibrissa, lower ring sinus, hair bulb, hair matrix, blood vessel, erythrocyte, and outer root sheath, respectively. Other abbreviations are the same as those used in previous figures. Samples in (**A–I**) were obtained from the mystacial pads of the animals on day 2 after birth, and those in (**J–L**) were obtained from the animals on day 5 after birth. (**A**) Control. (**B, C**) SMA staining. Thin arrows indicate the staining of muscle outside of the capsule and the thick arrows indicate the staining of the dermal sheath. The blue arrows show that no staining was observed in the dermal sheath associated with early stage vibrissal follicles. The asterisk in (**C**) designates a thin blood vessel. (**D**) SMA staining around the hair bulb of vibrissa. (**E**) Vimentin staining around the hair bulb of vibrissa. SMA (**F, H**) and vimentin (**G**) observed in a hair follicle of mystacial pad. (**I**) Enlarged view of the localization of SMA. (**J**) Control. (**K**) SMA staining. (**L**) Vimentin staining. Thick blue arrows in (**G, L**) indicated that the dermal sheath enclosing the hair bulb often lacks a vimentin signal, though it is distinct in the upper and middle area of the follicle as depicted by thick black arrows (**G**). Bars=200 μm (**B**), 100 μm (**A, C**), 50 μm (**D–H, J–L**), 30 μm (**I**).

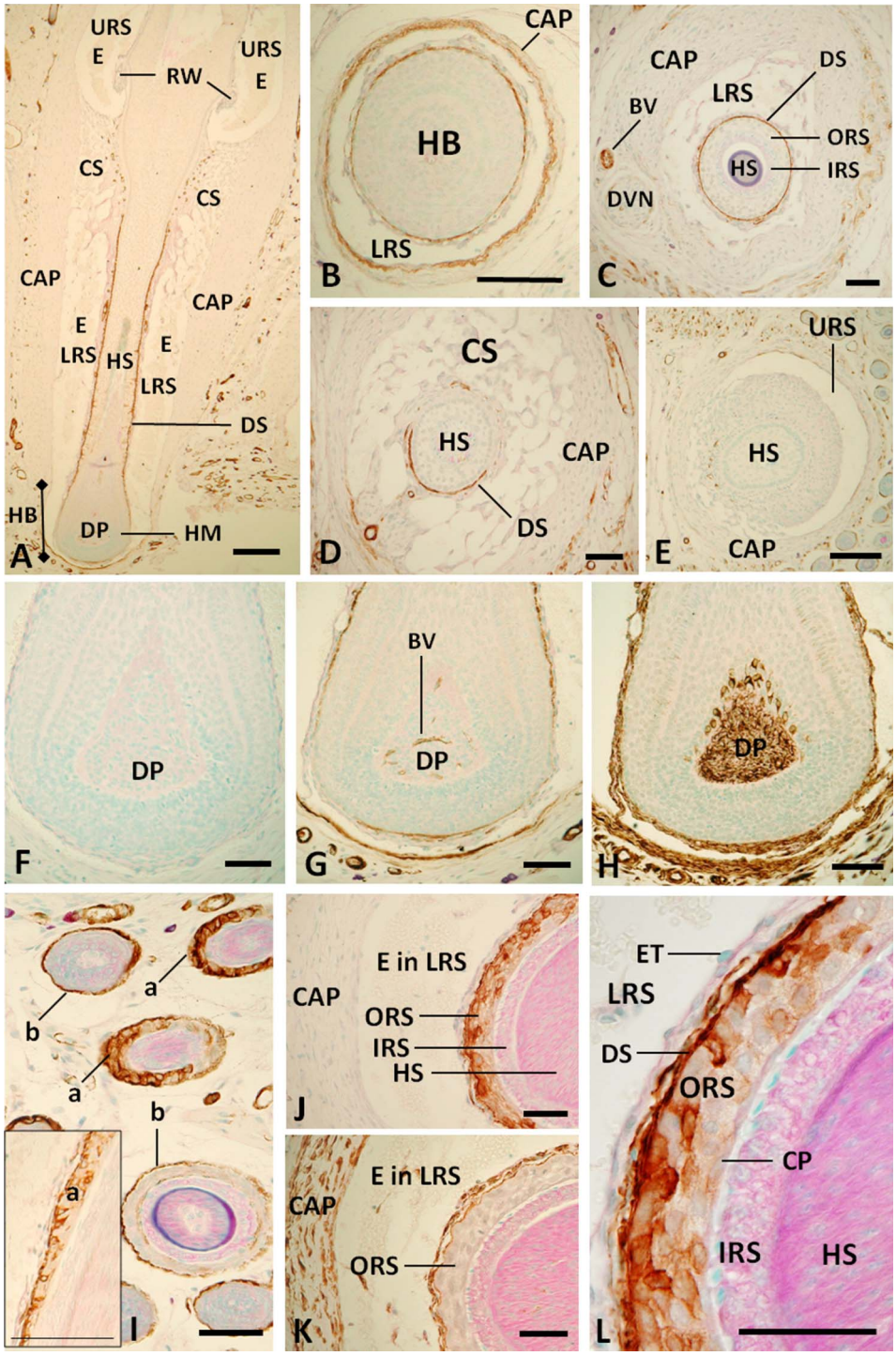

Fig. 7. Localization of SMA and vimentin in the mystacial pad of adult rats. Abbreviations: URS, upper ring sinus; LRS, lower ring sinus; CS, cavernous sinus; RW, ringwulst; E, erythrocyte; CAP, capsule of vibrissa; HS, hair shaft; DS, dermal sheath; DP, dermal papilla; HM, hair matrix; HB, hair bulb; ORS, outer root sheath; IRS, inner root sheath; CP, companion layer; DVN, deep vibrissal nerve; BV, blood vessel; ET, endothelium. Samples were obtained from the mystacial pad of rats on day 35 (**I–L**) after birth, on day 42 (**A**), on day 48 (**F–H**), and on day 61 (**I**, inset). Samples in (**B–E**) were obtained from young animals on day 7 after birth. (**A**) Localization of SMA in the vibrissal follicle. (**B–E**) Localization of SMA in the vibrissal follicle shown by the cross-sections at the levels of hair bulb (**B**), lower ring sinus (**C**), cavernous sinus (**D**), and upper ring sinus (**E**). Panels **F–H** are longitudinal views of hair bulbs. (**F**) Control. (**G**) SMA staining. (**H**) Vimentin staining. (**I**) SMA. a: Staining of outer root sheath. b: Staining of dermal sheath. (**J–L**) SMA staining at the level of lower ring sinus. (**K**) Vimentin staining at the level of lower ring sinus. Bars=200 μm (**A**), 100 μm (**B, E**), 50 μm (**C, D, F–I**, and insets in **I, J, K**), 30 μm (**L**).

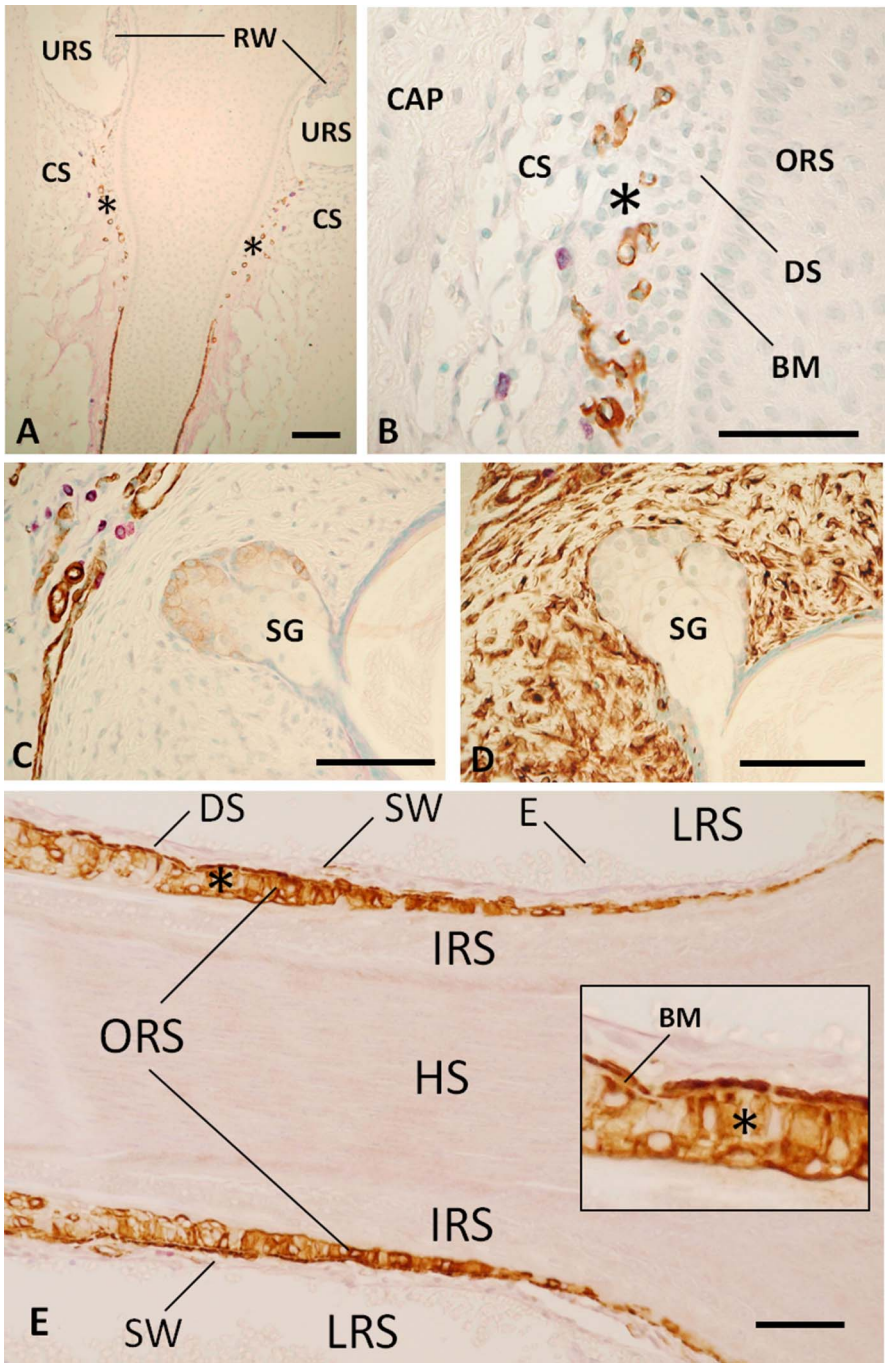

Fig. 8. Fine determination of the localization of SMA. Abbreviations: SG, sebaceous gland; SW, sinus wall; BM, basement membrane. Other abbreviations are the same as those described in the legend to Figure 7. (**B**) is an enlarged view of (**A**), focused at the area designated by the asterisks in (**A**). The asterisk in the inset figure of (**E**) shows the staining of the outer root sheath. Samples were obtained from the mystacial pad of the animals on day 35 (**B–D**), day 48 (**A**), and day 61 (**E**). The inset figure in (**E**) is the enlarged view of the area designated by the asterisk in (**E**). Bars=100 μm (**A**), 50 μm (**C–E**), 30 μm (**B**).

to have no distinct signal. The unstained gap, which is the basement membrane (designated as BM) between dermal sheath and outer root sheath, is observable in Figure 8B or in the inset figure of Fig. 8E. At approximately the same height as the cavernous sinus (CS), SMA staining appears to be discontinuous (asterisks in Fig. 8A and 8B), and recedes from the basement membrane (Fig. 8B). Therefore, whether stained cells in this area are a part of the dermal sheath is an unresolved question. The dermal sheath near the area higher than the CS typically has no SMA signal, except in the basal area of the sebaceous gland (Fig. 8C). The sebaceous gland showed no vimentin signal (Fig. 8D).

In contrast, the surrounding capsule tissue expressed a strong vimentin signal (Fig. 8D). No SMA signal was observed in the vibrissa capsule (Fig. 8C). Figure 8E shows distinct SMA-staining of the outer root sheath (see the area designated by the asterisk and also the inset figure) as well as that of the dermal sheath.

IV. Discussion

The pilosebaceous unit is a mammalian-specific organ and is composed of hair follicle, the sebaceous gland, and arrector pili muscle. The hair shaft is supported by many appendant tissues, such as the inner and outer root sheaths, basement membrane, dermal sheath, dermal papilla, sebaceous gland, and arrector pili muscle [3, 17]. The vibrissal hair is further supported by additional tissues: the thick capsule, sinus, nerve, and voluntary muscle [7]. Hair is dependent on these supporting tissues for their development, function, and maintenance. We investigated the localization of nonmuscle myosin and actin in the skin and found that these proteins are abundant in the outer root sheath of the hair follicle [19]. We examined the localization of SMA and vimentin expression in the hair-supporting tissues during and after the formation of the pilosebaceous unit.

The arrector pili muscle is attached to one or several hair follicles at the bulge area and plays a role in erecting the hair through contraction when animals feel cold or fear stress [14]. We examined the morphology and changes in arrector pili muscle using SMA immunohistochemistry. The results showed that (1) the arrector pili muscle is formed in the neonatal period and is completed by day 7 after birth, (2) the arrector pili muscle is maintained for a few weeks, after which cellular SMA levels decrease, and (3) the SMA decrease in the arrector pili muscle is more drastic in the ventral skin than in the dorsal skin. These results correlate with the need to protect neonatal animals from cold. The arrector pili muscle develops several days after birth because neonatal animals typically live under the coat of their mothers during the first week after birth but begin to explore the outer world thereafter. If the protected animal is able to reverse its posture and quickly face upward, ventral hair erection may not be important. A recent study by Zeveke and Shabanov showed that the deformation of the skin upon cooling is due to the contraction of collagen fiber bundles rather than the contraction of the smooth muscle of vessels or piloerectors in adult rats [33]. Their conclusion is consistent with our results, which show that the arrector pili muscle is deteriorated in adult rats.

In addition to these results, we examined the samples obtained from several different stages and from different skin positions. The results showed that distal end of the arrector pili muscle did not appear to be in contact with the basement membrane. Although the proximal ends of the arrector pili muscle are known to be connected to the bulge area of the hair follicle via elastic tendons [24], the attachment of the distal ends to the basement membrane has not been verified. Narisawa *et al.* reported that most of the distal ends were located in the upper dermis, while some seemed to be in close contact with the epidermal basal layers in the scalp skin of a 12-month-old human infant. They also observed a close topographic correlation between the distal ends of the arrector pili muscle and Merkel cells [22]. Clifton *et al.* showed results supporting the hypothesis that the distal ends of the arrector pili muscle may connect to the basement membrane via $\alpha 5\beta 1$ integrin, fibronectin, and the extracellular matrix in the human scalp skin [5].

SMA-positive tissue in the skin does not only include the arrector pili muscle. Other tissues, such as blood vessels, fetal or neonatal dermal muscles, dermal sheaths, outer root sheaths, and sebaceous glands also exhibit a positive SMA signal. Jahoda *et al.* observed SMA expression in the lower half of the dermal sheath [12]. We reexamined and confirmed their results in various developmental stages of rats. An exception was observed in immature follicles. Dermal cells surrounding immature hair follicles did not express SMA (Figs. 2B and 6H). We further presented results showing that some outer root sheath cells, located at the corresponding height of the SMA-positive dermal sheath, express an SMA signal. Our previous study suggested that the outer root sheath also expresses nonmuscle myosin and actin [19]. These energy-transducing proteins are thought to provide morphological stability and elasticity to the hair follicle. Since hair and vibrissal follicles are often forced to bend or flatten through routine contact of the shafts with external components or by inner contraction of dermal muscles, the hair root is thought to possess elasticity and toughness. We herein suggest that SMA located in the dermal sheath and outer root sheath reinforce the structures of hair-supporting tissues. SMA is detectable in fetal and neonatal dermal muscle; however, it decreases in adult animals. SMA is also detected in the basal area of the sebaceous gland. The signal is weak but detectable from neonatal to adult stages (Figs. 6 and 8). Interestingly, the outer wall of the ring sinus in the vibrissal follicle shows no SMA signal (Fig. 7A and 7J), except at the bottom area of the lower ring sinus surrounding the hair bulb (Fig. 7A and 7B). This SMA expression at the bottom of the vibrissal follicle may correlate with the thinness of the capsule in this area.

Vimentin is an intermediate filament protein expressed in mesenchymal tissues, particularly in connective tissues [6, 8] and in smooth muscles [29]. As shown in Figure 5, the dermal sheath is rich in vimentin. In contrast to SMA, vimentin in the dermal sheath is observed at all follicle heights and is often abundant in the dermal papilla. This suggests that vimentin is one of the basic components supporting the hair follicle, and that SMA has a special role in protecting the border area between soft and hard tissues. To produce force in smooth muscle, vimentin, as well as SMA, may be one of the essential elements [29]. In vibrissal follicles, vimentin appears to play an important role, since it was shown to be highly abundant in the capsule, which is the outermost robust tissue surrounding all other tissues of the vibrissal follicle (Figs. 7 and 8).

V. References

1. Animal Diversity Web, University of Michigan Museum of Zoolology. http://animaldiversity.ummz.umich.edu/site/topics/mammal_ anatomy/hair.html
2. Barcaui, C. B., Pineiro-Maceira, J. and De Avelar Alchorne, M. M. (2002) Arrector pili muscle: evidence of proximal attachment variant in terminal follicle of the scalp. *Br. J. Dermatol.* 146; 657–658.
3. Botchkarev, V. A. and Paus, R. (2003) Molecular biology of hair morphogenesis; development and cycling. *J. Exp. Zool.* 298B; 164–180.
4. Burgdorf, W. H. C., Plewig, G., Wolff, H. H. and Landthaler, M. eds. (2009) Braun-Falco's Dermatology, 3rd ed. Section 1, Springer Medizin Verlag Heidelberg.
5. Clifton, M. M., Mendelson, J. K., Mendelson, B., Montague, D., Carter, C., Smoller, B. R. and Horn, T. D. (2000) Immunofluorescent microscopic investigation of the distal arrector pili: A demonstration of the spatial relationship between $\alpha 5\beta 1$ integrin and fibronectin. *J. Amer. Acad. Dermatol.* 43; 19–23.
6. Coulombe, P. A., Olivier, B., Ma, L., Yamada, S. and Wirtz, D. (2000) The 'ins' and 'outs' of intermediate filament organization. *Trends Cell Biol.* 10; 420–439.
7. Ebara, S., Kumamoto, K., Matsuura, T., Mazurkiewicz, J. E. and Rice, F. L. (2002) Similarities and differences in the innervation of mystacial vibrissal follicle-sinus complexes in the rat and cat: a confocal microscopic study. *J. Comp. Neurol.* 449; 103–119.
8. Eriksson, J. E., Dechat, T., Grin, B., Helfand, B., Mendez, M., Pallari, H-M. and Goldman, R. D. (2009) Introducing intermediate filaments: from discovery to disease. *J. Clin. Invest.* 119; 1763–1771.
9. Gumbiner, B. M. (1996) Cell adhesion: the molecular basis of tissue architecture and morphogenesis. *Cell* 84; 345–357.
10. Halal, J. (2008) Hair Structure and Chemistry Simplified, 5th ed. Milady Pub. Corp.
11. Hardy, M. H. (1992) The secret life of the hair follicle. *Trends Genet.* 8; 55–61.
12. Jahoda, C. A. B., Reynolds, A. J., Chaponnier, C., Forester, J. C. and Gabbiani, G. (1991) Smooth muscle α-actin is a marker for hair follicle dermis in vivo and in vitro. *J. Cell Sci.* 99; 627–636.
13. Lam, E. M., Worrell, G. A. and Laughlin, R. S. (2010) Semiology of the rare seizure subtype piloerection. *Arch. Neurol.* 67; 1524–1527.
14. Masuda, Y., Suzuki, M., Akagawa, Y. and Takemura, T. (1999) Developmental and pharmacological features of mouse emotional piloerection. *Exp. Anim.* 48; 209–211.
15. Mittal, S., Oni-Orisan, A., Stenz, J. and Shah, A. K. (2010) Temporal neocortical origin of pilomotor seizures in association with an infiltrating glioma: a case confirmed by intracranial electroencephalography monitoring. *J. Neurosurg.* 113; 388–393.
16. Miyake, Y., Inoue, N., Nishimura, K., Kinoshita, N., Hosoya, H. and Yonemura, S. (2006) Actomyosin tension is required for correct recruitment of adherens junction components and zonula occudens formation. *Exp. Cell Res.* 312; 1637–1650.
17. Morioka, K. (2005) Hair Follicle: Differentiation under Electron Microscope. Springer Verlag Tokyo.
18. Morioka, K. (2009) A guide to hair follicle analysis by transmission electron microscopy: technique and practice. *Exp. Dermatol.* 18; 577–582.
19. Morioka, K., Matsuzaki, T. and Takata, K. (2006) Localization of myosin and actin in the pelage and whisker hair follicles of rat. *Acta Histochem. Cytochem.* 39; 113–123.
20. Morioka, K., Sato-Kusubata, K., Kawashima, S., Ueno, T., Kominami, E., Sakuraba, H. and Ihara, S. (2001) Localization of cathepsin B, D, L, LAMP-1 and μ-calpain in developing hair follicles. *Acta Histochem. Cytochem.* 34; 337–347.
21. Narisawa, Y. and Kohda, H. (1993) Arrector pili muscles surround human facial vellus hair follicles. *Br. J. Dermatol.* 129; 138–139.
22. Narisawa, Y., Hashimoto, K. and Kohda, H. (1996) Merkel cells participate in the induction and alignment of epidermal ends of arrector pili muscles of human fetal skin. *Br. J. Dermatol.* 134; 494–498.
23. Poblet, E., Ortega, F. and Jimenez, F. (2002) The arrector pili muscle and the follicular unit of the scalp: A microscopic anatomy study. *Dermatol. Surg.* 28; 800–803.
24. Rodrigo, G. F., Cotta-Pereira, G. and David-Ferreira, J. F. (1975) The fine structure of the elastic tendons of the arrector pili muscle. *Br. J. Dermatol.* 93; 631–636.
25. Shin, I. S., Park, N. H., Lee, J. C., Kim, K. H., Moon, C., Kim, S. H., Shin, D. H., Park, S. C., Kim, H. Y. and Kim, J. C. (2010) One-generation reproductive toxicity study of epichlorohydrin in Sprague-Dawley rats. *Drug Chem. Toxicol.* 33; 291–301.
26. Song, W-C., Hu, K-S., Kim, H-J. and Koh, K-S. (2007) A study of the secretion mechanism of the sebaceous gland using three-dimensional reconstruction to examine the morphological relationship between the sebaceous gland and the arrector pili muscle in the follicular unit. *Dermatopathology* 157; 325–330.
27. Song, W-C., Hwang, W-J., Shin, C. and Koh, K-S. (2006) A new model for the morphology of the arrector pili muscle in the follicular unit based on three-dimensional reconstruction. *J. Anat.* 208; 643–648.
28. Standring, S. ed-in-chief. (2008) Gray's Anatomy, 40th ed. Chapter 7, Elsevier Limited.
29. Tang, D. D. (2008) Intermediate filaments in smooth muscle. *Am. J. Pysiol. Cell Physiol.* 294; C869–C878.
30. Vidal, I. (2009) Piloerection: a side effect of intravenous administration of dobutamine. *Arq. Bras. Cardiol.* 92; 290–293.
31. Wang, M., Shu, B., Bai, W. X., Liu, J., Yao, J., Pan, W. N. and Pan, Y. Y. (2010) A 4-week oral toxicity study of an antiviral drug combination consisting of arbidol and acetaminophen in rats. *Drug Chem. Toxicol.* 33; 244–253.
32. Wolff, K., Goldsmith, L. A., Katz, S. I., Gilchrest, B. A., Paller, A. S. and Jeffel, D. J. eds. (2008) Fitzpatrick's Dermatology in General Medicine, 7th ed. Section 15, The McGraw-Hill Companies, Inc.
33. Zeveke, A. V. and Shavanov, D. V. (2010) A study of skin deformation by optical coherence microscopy. *Biophysics* 55; 301–304.